frontiers | Frontiers in Malaria

TYPE Original Research
PUBLISHED 28 November 2024
DOI 10.3389/fmala.2024.1484359

OPEN ACCESS

EDITED BY
Marion Avril,
MalarVx, United States

REVIEWED BY
Justin Yai Alamou Doritchamou,
National Institute of Allergy and Infectious Diseases (NIH), United States
Nancy Odurowah Duah-Quashie,
University of Ghana, Ghana

*CORRESPONDENCE
Hernando A. del Portillo
hernandoa.delportillo@isglobal.org
Eliana M. Arango-Flórez
eliana.arango@udea.edu.co

RECEIVED 21 August 2024
ACCEPTED 22 October 2024
PUBLISHED 28 November 2024

CITATION
Martínez-Moreno JA, Ayllon-Hermida A, Barnadas-Carceller B, Fernández-Becerra C, del Portillo HA, Carmona-Fonseca J and Arango-Flórez EM (2024) Proteomic profile of plasma-derived extracellular vesicles from Colombian pregnant women with *Plasmodium*-soil transmitted helminths coinfection. *Front. Malar.* 2:1484359. doi: 10.3389/fmala.2024.1484359

Proteomic profile of plasma-derived extracellular vesicles from Colombian pregnant women with *Plasmodium*-soil transmitted helminths coinfection

Jahnnyer A. Martínez-Moreno[1], Alberto Ayllon-Hermida[2,3,4], Berta Barnadas-Carceller[2,3], Carmen Fernández-Becerra[2,3,5], Hernando A. del Portillo[2,3,6]*, Jaime Carmona-Fonseca[1] and Eliana M. Arango-Flórez[1,7]*

[1]Grupo Salud y Comunidad-César Uribe Piedrahíta, Facultad de Medicina, Universidad de Antioquia, Medellín, Colombia, [2]ISGlobal, Hospital Clínic, Universitat de Barcelona, Barcelona, Spain, [3]Instituto de Investigación Germans Trias I Pujol (IGTP), Germans Trias i Pujol Health Research Institute, Badalona, Spain, [4]School of Medicine and Health Sciences, University of Barcelona, Barcelona, Spain, [5]Centro de investigación Biomédica en Red Enfermedades Infecciosas (CIBERINFEC), Instituto de Salud Carlos III (ISCIII)-CIBER de Enfermedades Infecciosas, Instituto de Salud Carlos III, Madrid, Spain, [6]Institución Catalana de Investigación y Estudios Avanzados, Catalan Institution for Research and Advanced Studies (ICREA), Barcelona, Spain, [7]Grupo de Investigación en Enfermedades Infecciosas y Crónicas-GEINCRO, Facultad de Ciencias de la Salud, Fundación Universitaria San Martín, Sabaneta, Colombia

Introduction: Extracellular vesicles (EVs) are lipid bilayer membrane-enclosed nanoparticles, secreted by all cell types. Information regarding EVs and their molecular cargo in gestational parasitic infections, particularly those caused by *Plasmodium* and soil-transmitted helminths (STH), remains largely unexplored. This study aimed to perform isolation and molecular characterization of plasma-derived EVs from Colombian pregnant women and compare quantity, size, concentration and protein cargo of those EVs according to the infectious status, to investigate if parasite-derived proteins could be detected as biological cargo of circulating EVs of pregnant women infected with *Plasmodium*, STH and co-infections.

Materials and methods: A descriptive study with 5 groups was performed: 1) Pregnant women with *Plasmodium* infection (n=10). 2) Pregnant women with STH infection (n=14). 3) Pregnant women with coinfection *Plasmodium* and STH (n=14). 4) Pregnant women without infection with *Plasmodium* nor STH (n=10). 5) Non-pregnant women without infection with *Plasmodium* nor STH (n=6). Plasma-derived EVs were isolated by size exclusion chromatography (SEC) and fractions containing EVs identified by a bead-based flow cytometric assay for CD9; the size and concentration of EVs were quantified by nanoparticle tracking analysis, and proteins associated with EVs were identified by liquid chromatography-mass spectrometry in a pool of samples per study group.

Results: There were no statistical differences in expression of the CD9 EVs marker among study groups. The size range of EVs was more variable in the three infected groups (100-700 nm) compared to the size range of the uninfected

groups (50-300 nm). A total of 823 quantifiable proteins with measurable abundance values were identified within the five study groups. Of the total quantifiable proteins, 758 were identified as human, six proteins pertained to *P. vivax*, fifteen to *Trichiuris trichiura*, and one to hookworms. Data are available via ProteomeXchange with identifier PXD051270.

Discussion: This is the first study that identifies proteins from *Plasmodium* and STH in EVs isolated from pregnant women. The identification of such proteins from neglected tropical parasites accounting for a major burden of disease worldwide, open the possibilities of studying their physiological role during infections as well as exploring them for antigen discovery, vaccine development and biomarker discovery.

KEYWORDS

extracellular vesicles, proteomics analysis, pregnant women, *Plasmodium*, soil-transmitted helminths, Colombia

1 Introduction

Parasitic infections are an important cause of global morbidity and mortality and are prevalent in low- and middle-income countries, where it is estimated that more than 1,000 million people suffer from parasitic infections, which generate strong social and economic impacts (Utzinger et al., 2012). Among these, malaria and soil-transmitted helminth (STH) infections are of great importance due to their high frequency and wide distribution, mainly in regions of East Asia, sub-Saharan Africa and Latin America (Lustigman et al., 2012; Murray et al., 2014), where socioeconomic and eco-epidemiological conditions are favorable for the spread of these infections that usually co-infect humans (Alvarez-Larrotta et al., 2018).

Pregnant women and children under 5 years old are at the highest risk for complications of parasitic infections, impacting both pregnancies and newborn health (Rogerson et al., 2007b; Blackwell, 2016; Banco Interamericano de Desarrollo et al., 2011; White et al., 2014; Blackwell, 2016; Honkpéhèdji et al., 2021; Mpairwe et al., 2014). The increased risk in pregnant women is linked, at least in part, to the immune tolerance status present during pregnancy (Saito et al., 2010). Thus, during the maternal-fetal interface, the anti-inflammatory (Th2) and anti-inflammatory-regulatory immunological responses (Treg) predominate, while keeping the pro-inflammatory (Th1-Th17) response controlled, but not absent. However, this predominance or excess of the anti-inflammatory and regulatory response during pregnancy can increase the frequency of symptomatic and severe infections such as malaria and STH in pregnant women (Jamieson et al., 2006; Saito et al., 2010).

The acute immune response to malaria parasites is proinflammatory with an increase in cytokines such as TNFα, IFNγ, IL-12, IL-23, and IL-17 (Crompton et al., 2014; Rogerson et al., 2007a). However, repeated exposure to malaria parasites, particularly in low parasitaemia, results in the development of an "anti-disease" immunity, which is defined by tolerance to the parasite and characterized by a predominant Th2/Treg immune profile (Álvarez-Larrotta et al., 2019; Freitas do Rosario and Langhorne, 2012; Minigo et al., 2009; Wammes et al., 2013).

On the other hand, in the context of helminth infections, a response characterized by the presence of a Th2 immune profile is stablished, accompanied by an immunoregulatory response. This, lead to hyperreactivity of immune cells and expansion of T-reg cells, which collectively contribute to the chronicity of the infection (Gazzinelli-Guimaraes and Nutman, 2018).

Other mediators that have recently been described as immunomodulators during infections caused by *Plasmodium* and helminths—including several STH—are extracellular vesicles (EVs) (Marcilla et al., 2014; Sampaio et al., 2017). EVs are nanoparticles structurally formed from bilipid membranes, with an important role in intercellular communication in eukaryotes (Yáñez-Mó et al., 2015; Jeppesen et al., 2023). Their cargo is heterogeneous (proteins, lipids, nucleic acids and metabolites), as well as their size and biogenesis (exosomes, microvesicles, oncosomes and apoptotic bodies), and they are secreted by cells into different biological fluids such as serum, plasma, cerebrospinal fluid, among others (Mathieu et al., 2019). Thus, indicating their potential as novel biomarkers of disease, including parasitic infections (Fuhrmann et al., 2017).

Several recent investigations have described the production of EVs during *Plasmodium* or helminth infections, attributing them multiple functions to modulate the immune response (Buck et al., 2014; Martin-Jaular et al., 2011; Martín-Jaular et al., 2016; Sánchez-López et al., 2024) and in the pathogenesis of the disease (Debs et al., 2019; Dekel et al., 2021; Sisquella et al., 2017). However, only one study is presently available on the human micro-RNA cargo of EVs

during pregnancy in malaria (Moro et al., 2016), while none studies have been reported on the protein cargo of EVs in the context of coinfection by *Plasmodium* and STH in pregnant women.

This study aimed to carry out the isolation and molecular characterization of plasma-derived EVs from pregnant women residing in Colombian territories co-endemic for *Plasmodium* and STH infections, according to the infection status of the pregnant women.

2 Materials and methods

2.1 Ethical aspects

Individual written informed consent was obtained from all study participants before the collection of samples, after receiving oral and written complete information about study objectives and procedures. The project was approved by the Ethics Committee of the Medical Research Institute of the University of Antioquia (committee 010 of May 14, 2019). The confidentiality of the information was guaranteed by using an alphanumeric code to identify the samples of each participant. The protocol for sample collection and research procedures was governed by the provisions of Resolution No. 008430 of 1993 of the Ministry of Health of Colombia.

2.2 Design, study groups and sample size

Descriptive, prospective and cross-sectional study, with convenience sampling, of pregnant women residing in Puerto Libertador, Tierralta or Quibdó. Five study groups were defined according to the presence of pregnancy and *Plasmodium* and STH infection:

1. Pregnant women with *Plasmodium* infection (*P. falciparum* or *P. vivax*) (P; n=10)
2. Pregnant women with STH infection (G; n=14)
3. Pregnant women with coinfection with *Plasmodium* and STH (PG; n=14)
4. Pregnant women without infection with *Plasmodium* nor STH: Control (C; n=10).
5. Non-pregnant women without infection with *Plasmodium* nor STH: Control (NG; n=6).

2.3 Inclusion and exclusion criteria

The women were ascribed to the research between 2016-2022 in the obstetric units of the hospital establishments in the municipalities of Puerto Libertador and Tierralta in the south of the department of Córdoba, and Quibdó, in the department of Chocó, which are endemic for malaria and STH (Carmona-Fonseca, 2020; Ministerio de Salud y Protección Social, U. de A, 2015).

The women were permanent residents of the study area at the time of delivery, with prenatal care and delivery attended at the respective local hospital. In addition, they did not present other infections according to the results of the tests for TORCHS and HIV, nor diseases such as high blood pressure, gestational diabetes, preeclampsia-eclampsia, kidney failure, asthma, and they reported a negative result in a serological test for acute dengue virus infection.

The only exclusion criteria were withdrawal of informed consent and failure to obtain samples to diagnose the infectious status.

2.4 Data and sample collection

After inclusion, a questionnaire was completed for each woman to record demographic, clinical, and epidemiological data.

At the time of delivery, peripheral blood samples from the pregnant woman and the placenta were collected in tubes with ethylenediaminetetraacetic acid (EDTA) to make the microscopic diagnosis of plasmodial infection using thick blood smears (TBS). In parallel, fractions of the blood samples were placed on Whatman #3 filter paper for the molecular diagnosis of *Plasmodium* infection by real-time quantitative PCR (qPCR) (Arango et al., 2013). Additionally, participants were asked for a single sample of approximately 3 g of feces. A fraction of this sample was used to determine the presence of STH (*Ascaris lumbricoides, Trichiuris trichiura*, and *Necator americanus/Ancylostoma duodenale*-hookworms) through direct and concentration fecal examinations. The other fraction was used to validate the absence of STH by PCR in the negative samples by microscopy.

2.5 Determination of infectious status

The microscopic diagnosis of plasmodial infection was performed by an experienced microscopist in each local hospital, following the criteria suggested by the WHO (World Health Organization, 2023). A thick smear was considered negative when no parasitic form was observed in a minimum of 200 microscopic fields.

The extraction of parasite DNA for the molecular diagnosis of plasmodial infection was carried out with the QIAamp® DNA Mini kit (QIAGEN) following the manufacturer's instructions. The diagnosis was made from blood samples collected on Whatmann #3 filter paper. For this, a 6 mm diameter circle was used (~25 µL of blood) and the DNA obtained was resuspended in 50 µL of molecular grade water. qPCR was performed following a previously described procedure (Alvarez-Larrotta et al., 2018; Gavina et al., 2017). Briefly, samples were first analyzed for *Plasmodium* DNA using genus-specific primers and a hydrolysis probe (Plasprobe). Samples with a cycle threshold (Ct) <45 were analyzed in two species-specific reactions for *P. falciparum* and *P. vivax*. Only those samples positive in both genus and species were considered positive. *P. vivax* (DNA from the Salvador I strain) and *P. falciparum* (DNA from the 3D7 strain) were used as positive controls. Cycling and detection were performed in the Applied Biosystems StepOnePlus™ real-time PCR system under universal amplification conditions.

Direct fecal smears and concentration examinations (Ritchie-Frick method) for STH diagnosis were carried out by expert professionals from the Parasitology group of the Faculty of Medicine of the

University of Antioquia. The number of eggs per gram of feces was calculated to estimate the intensity of infection (Barreto et al., 2017). For molecular diagnosis of STH, DNA was extracted from 200 mg of feces using the Stool DNA Isolation kit (Norgen) and following the manufacturer's instructions; subsequently a qPCR-Taqman assay was performed according to other authors (Basuni et al., 2011; Sow et al., 2017), in order to validate the absence of *A. lumbricoides, T. trichiura, N. americanus/A. duodenale*. Cycling and detection were performed in the Applied Biosystems StepOnePlus™ real-time PCR system under universal amplification conditions.

2.6 Analysis of plasma-derived EVs

From each participant, 6 mL of whole blood was collected by venipuncture, deposited in Vacutainer tubes (BD Biocienses) with EDTA. The tubes were centrifuged at 400 × g for 10 minutes at room temperature; the entire volume of plasma obtained was collected (approx. 2 mL) and fractionated into 2 mL aliquots to be stored and subsequently frozen at -80°C. The study and characterization of EVs was carried out in the *Plasmodium vivax* and Exosome Research Group (PvREX) (https://www.pvrex.org/) of the Barcelona Institute for Global Health (ISGlobal) and the Germans Trias i Pujol Research Institute (IGTP) (Badalona, Barcelona, Spain), following sequential steps (Supplementary Figure 1).

2.7 Isolation of EVs by size exclusion chromatography (SEC)

EVs were isolated and purified from plasma samples under sterile conditions using class II biosafety hoods. In brief, the plasma was thawed on ice and then centrifuged twice for 10 minutes at 4 °C, first at 2000 × g, and then at 8000 × g, to eliminate cellular debris and excess lipids present in the sample. Sepharose columns were prepared according to previously established protocols (de Menezes-Neto et al., 2015). Briefly: i) a nylon mesh of approximately 1 cm^2 (filter) was introduced into the needle pivot of sterile syringes; ii) Sepharose CL-2B (Sigma–Aldrich) was packed into the syringes to a final volume of 10 mL by plugging the needle pivot with a three-way valve; iii) it was left to decant overnight at 4°C; iv) then, the columns were equilibrated by adding 10 mL of sterile 1X Phosphate Buffered Saline (PBS) used as elution buffer. Once all the elution buffer passed through the column by gravitation, without allowing the Sepharose column to dry, approximately 1 mL of the plasma, previously centrifuged, was loaded onto each column and fourteen fractions of 500 µL each were collected immediately using sterile 1X PBS, for that, the column was topped up with PBS intermittently during the acquisition of the fourteen fractions of 500 µL. Concentration of soluble proteins, mostly contaminants, contained in the fractions collected after chromatography was measured using the Pierce™ BCA Protein Assay Kit (Thermo Scientific) following the manufacturer's instructions. The fractions were aliquoted and frozen at -80°C until use in subsequent assays.

2.8 Identification and molecular characterization of EV-enriched fractions by bead-based flow cytometry assay (BBA) for CD9

We used a bead-based flow cytometry assay (BBA) to identify SEC fractions enriched in the classic EV marker, CD9 (Martin-Jaular et al., 2011; de Menezes-Neto et al., 2015). Briefly, 45 µL of each fraction was mixed with 5 µL of 4 µm aldehyde/sulfate-latex beads (Invitrogen) prediluted 1:10 in 1X PBS, and incubated for 15 minutes at room temperature. As a negative control, 45 µL of 1X PBS was added instead of samples. Coupled beads were blocked by incubation overnight with 1 mL of bead-coupling buffer (BCB), consisting of PBS with 0.1% bovine serum albumin and 0.01% NaN_3, at room temperature with rotation. EV-coupled beads were then centrifuged at 5000 × g for 10 minutes at room temperature, washed once with BCB, and resuspended in 250 µL of BCB before incubation with the primary antibody.

For primary staining of EVs, 5 µL of antibodies against CD9 tetraspanin (Mouse-anti-CD9 human; clone VJ1/20 (Immunostep S.L-9PU-01MG) 1:500 dilution was mixed with 45 µL of sample (EV + beads) in 96-well round bottom dishes and incubated for 30 minutes at 4°C. After incubation and washing, plates were centrifuged at 2500 × g for 10 minutes. Immediately, EV-coupled beads were resuspended in 50 µL of Goat F(ab)2 anti-Mouse IgG (H+L) Human ads-FITC polyclonal secondary antibody (Southern Biotech-1032-02) and incubated in the dark for 30 minutes at 4°C. Subsequently, plates were washed twice with 150 µL of BCB, and centrifuged at 2500 × g for 10 minutes. As a negative staining control (Control), the EV-coupled beads of each fraction were incubated only with secondary antibody. Finally, stained beads were resuspended in 100 µL of 1X PBS and acquisition and reading were performed on the BD FACSLyricTM flow cytometer (BD Biosciences). One hundred beads for each sample were obtained in the cytometer. Analyzes were performed using FlowJo software version 10.6.1 to compare the median fluorescence intensity (MFI) of the EV-coupled beads, thereby measuring the amount of EVs.

2.9 Characterization of size and concentration of EVs by nanoparticle tracking analysis (NTA)

The NanoSight LM10 (Malvern Instruments Ltd) equipped with a 638 nm laser and a coupled camera (model F-033) was used. Data were analyzed with NTA software version 3.1, setting the detection threshold to 5, and the blur and maximum jump distance to automatic. To carry out the measurements, fraction obtained by SEC from each plasma sample, with the highest EV enrichment observed in the BBA, was diluted 1:10 with sterile 1X PBS. Readings were taken with single capture for 60 seconds at 30 frames per second (fps), with a camera level set to 16 and with manual temperature monitoring.

2.10 Identification of protein cargo of EVs by liquid chromatography/mass spectrometry (LC-MS)

For the proteomic analysis of the EVs of each study group, the procedure was as follows: first, 5 samples were randomly selected from the total samples of each study group and 200 µL of the SEC fraction were taken from each of the 5 selected samples more enriched with EVs according to the BBA assay for CD9 (faction with the highest MFI peak), to make a final mixture with a volume of 1 mL for each study group (Table 1). The proteins were then precipitated in the 5 mixtures, for which 250 µL of cold acetone (-20°C) was added to each mixture and incubated for 1 hour at -20°C, and then the proteins were recovered by centrifugation at 16000 × g for 15 minutes at 4°C. The precipitated proteins were processed to carry out the digestion and purification of peptides with the commercial iST kit (PreOmics), according to the manufacturer's instructions. Finally, they were sent for analysis to the Proteomics Unit of the Center for Genomic Regulation (CRG) of Barcelona-Spain. One µg of each sample was analyzed by LC-MS using a 90-minute gradient on the Orbitrap Eclipse mass spectrometer (Thermo Fisher Scientific). As a quality control, bovine serum albumin samples were analyzed between each sample to avoid carryover and evaluate instrument performance. Data are available via ProteomeXchange with identifier PXD051270.

2.10.1 Human proteomic analysis

Proteomic data were analyzed to assess the number of quantifiable human proteins and peptides per sample, along with the distribution of proteins based on peptide counts. The data were then filtered to include only human proteins, removing contaminants (keratin proteins), and excluding proteins identified by fewer than two unique peptides (UP). Only quantifiable proteins with measurable abundance were included in further analysis. The filtered proteins were compared to the top 100 proteins listed in Vesiclepedia (Chitti et al., 2024; Kalra et al., 2012; Pathan et al., 2019). Venn diagrams were generated with InteractiVenn (Heberle et al., 2015), and heatmaps displaying protein abundances across samples were created using TBTools (Chen et al., 2023). Gene Ontology (GO) annotation and Kyoto Encyclopedia of Genes and Genomes (KEGG) pathway enrichment analyses were conducted for proteins identified exclusively in infected samples using the Database for Annotation, Visualization and Integrated Discovery (DAVID) (Huang et al., 2008, 2009).

2.10.2 Parasite proteomics analysis

Raw mass spectrometry data files were analyzed with the Mascot database search algorithm v2.6 (http://www.matrixscience.com) using the UniProt proteome databases: *P. vivax*_UP00000833, *P. falciparum*_UP000001450, *Ancylostoma*_UP000054047, *Ascaris*_UP000036681, *Necator*_UP000053676 and *Trichuris*_UP000030665, and protein/peptide identification was performed using Proteome Discoverer v2.5 software (Thermo Fischer Scientific). Peptides have been filtered based on: (i) minimum peptide length of 7; (ii) maximum false discovery rate (FDR) for peptides and proteins of 1%; (iii) minimal peptides per protein of 1 and minimal unique peptides per protein of 1. The candidate proteins for validation have been filtered by eliminating those proteins that appear in the samples from uninfected participants (false positives).

2.11 Statistical analysis

The variables median fluorescence intensity, EVs size, EVs concentration, soluble protein concentration and others do not have a Gaussian distribution according to the Kolmogorov-Smirnov test, therefore, the non-parametric Kruskal-Wallis (KW) ANOVA test was used to compare the medians of the five study groups. If this test showed a significant difference ($p<0.05$), Dunn's test for multiple comparisons was used to identify pairs of groups that differ statistically. The analyzes were done with the GraphPad Prism 8.0.1 program.

3 Results

3.1 General characteristic of the women

Young women (15 to 42 years and median 20 to 25.8 years), height (median between 156 and 158 cm), weight (median between 58 and 61 kg among four groups and 71.8 kg in the fifth, pregnant women without infection), with hemoglobin with median values between 10.8 and 12.6 g/dL, but which is lower in women with an infection compared to those without infection. None of these four variables has a significant difference between the five study groups, but it is clear that infected pregnant women have less than 12 g/dL of hemoglobin, while non-infected women have 12 or more g/dL of hemoglobin, a situation that is clinically important (Table 2).

3.2 Comparison of the amount of EVs according to infection status

To determine the SEC fractions in which EVs were enriched, a bead-linked flow cytometry assay or BBA was performed using a classic EV biomarker such as tetraspanin CD9; median fluorescence intensity (MFI) was measured. An illustrative result of the determination of MFI for each of the study groups is shown in Supplementary Figure 2A. The set of results obtained demonstrated the presence, with variable intensity, of tetraspanin CD9 in all samples in each of the study groups. It was also observed that in more than 90% of the samples evaluated, the highest peak of CD9 expression was obtained in SEC fractions 6 or 7, which demonstrates consistency and homogeneity in the preparation of columns and the elution of fractions ensuring the reproducibility and homogeneity of the EVs isolated in the different samples. In all of the samples evaluated, an abundant content of soluble proteins was not found in the fractions where the highest peak MFI was obtained for CD9 (indicator of the amount of EVs). We determined if there was any difference in the expression of CD9 between the five groups evaluated and, although there were no significant differences

10.3389/fmala.2024.1484359

TABLE 1 Samples and fractions selected and mixed for proteomic analysis.

Study group	Woman code	SEC fraction with highest MFI for CD9	Parasitic species (parasite load)	Fever
Pregnant women without infection (C)	H90137	F7	N/A	No
	H8004	F6	N/A	No
	H8022	F7	N/A	No
	H8042	F6	N/A	No
	H8051	F7	N/A	No
Pregnant women with STH infection (G)	H8034	F7	Hookworms (500 e.p.g)	No
	H90142	F6	*A. lumbricoides* (500 e.p.g)	No
	H90143	F6	*T. trichiura* (500 e.p.g); Hookworm (500 e.p.g)	No
	H8002	F6	*T. trichiura* (500 e.p.g); Hookworm (500 e.p.g)	No
	H8015	F6	Hookworms (1000 e.p.g)	No
Pregnant women with Plasmodium infection (P)	H90111	F7	*P. vivax* (6311 p/μL)	Yes
	H90113	F7	*P. falciparum* (1814 p/μL)	Yes
	H90112	F6	*P. vivax* (7885 p/μL)	Yes
	H90121	F6	*P. vivax* (no data)	Yes
	H90118	F7	*P. vivax* (6266 p/μL)	Yes
Pregnant women coinfected (PG)	H9023	F6	Hookworms (1000 e.p.g); *P. falciparum* (29768 p/μL)	Yes
	H90116	F6	*T. trichiura* (500 e.p.g); Hookworms (1500 e.p.g); *P. vivax* (6243 p/μL)	Yes
	H90117	F6	*A. lumbricoides* (7500 e.p.g); *P. vivax* (212 p/μL)	Yes
	H90122	F6	*T. trichiura* (500 e.p.g); *P. falciparum* (240 p/μL)	Yes
	H8012	F6	Hookworms (500 e.p.g); *P. vivax* (18800 p/μL)	Yes
Non-pregnant women (NG)	H90199	F9	N/A	No
	H90198	F5	N/A	No
	H90200	F7	N/A	No
	H90201	F6	N/A	No
	H90202	F7	N/A	No

SEC, size-exclusion chromatography; MFI, median fluorescence intensity; STH, soil-transmitted helminths; F, fraction of SEC. N/A, Not applicable; e.p.g, eggs per gram of feces; p/μL, parasites per microliter.

(p=0.732), there was a tendency to show a higher value of MFI in the expression of CD9 in pregnant women with *Plasmodium* infection (P) followed by STH infection (G), compared to the other groups (Supplementary Figure 2A).

3.3 Characterization of EVs in pregnant women according to infection status

Nanoparticle tracking analysis (NTA) measures the number of particles per mL and the variation in their size. To apply the NTA, the fractions with the highest expression of CD9 in each sample, that is, those richest in EVs, were chosen (Supplementary Figure 2B). In general, a more heterogeneous size distribution of the nanoparticles was observed in the EV fractions of the groups of pregnant women with some infection (G, P or PG) compared to the control groups (C and NG). Furthermore, it could be seen that most of the EVs in the C and NG control groups are concentrated in a size range between 50 and 300 nm, while in the groups with some infection the size range was much more variable, between 100 and 700 nm (Supplementary Figure 2B).

To determine these possible differences in quantity and size, the groups were compared according to the concentration of particles per mL (Figure 1A) and their median size (Figure 1B) in each of the groups. When looking into the concentration of particles per mL, the lowest concentration is in the control group NG followed very closely by control group C; the three infected groups (P, G, PG) have values that are 2.5 times or more than the controls and are very similar between them, Interestingly, an slightly higher concentration of particles have been detected in PG coinfection

10.3389/fmala.2024.1484359

TABLE 2 General characteristics of women in each study group.

Variables (Me; IR)	Infected pregnant women			Un-infected women		p (KW)
	Plasmodium (P) n=10	STH (G) n=14	Co-infected (PG) n=14	Pregnant (C) n=10	Non-pregnant (NG) n=6	
Age (years old)	23.5; 9.5	24.5; 8.5	20; 5	24; 11.5	25;8	0.265
Height (cm)	158; 5	156; 5.5	157;5	156; 9.5	158;4	0.636
Weight (g)	61; 21	58; 10	60.2; 13.5	71.8; 5.75	58;16	0.255
Hemoglobin (g/dL)	10.8; 1.8	11.6; 2.3	10.9; 1.7	12; 0.68	12.6; 0.9	0.088

Me, median; IR, interquartile range; STH, soil-transmitted helminths; KW, Kruskall-Wallis test.

(Figure 1A), but there is no statistically significant differences between the groups (p=0.105), probably due to their small sample size. Then, analyzing the median size of the particles in each sample, particles detected ranged between ≈120 nm and ≈200 nm. The lowest values correspond to NG group and the highest to G group. Among the infected, the largest size is for G with no difference between P and PG (p=0.118) (Figure 1B). Though, we were able to observe that the particles purified by the SEC, independently from the sample analyzed, have a median size range corresponding to exosomes.

3.4 Identification of human proteins in plasma-derived EVs

A total of 823 quantifiable proteins with measurable abundance values were identified within the five study groups. The group of non-pregnant women (NG) with 553 proteins and pregnant women infected with *Plasmodium* (P) with 522 proteins were the ones that showed the highest number of proteins associated with EVs, compared to the other three: healthy pregnant women (C) 449, pregnant women with STH (G) 423 and pregnant women with coinfection (PG) 328 (Supplementary Figure 3).

Of the total quantifiable proteins, 758 were identified as human. After filtering, 11 keratins were excluded as contaminants, resulting in 561 human proteins with at least two unique peptides (UP) per protein group being included in the final EV proteome dataset (Figure 2A). Comparison with the top 100 most commonly identified EV proteins in Vesiclepedia revealed that 77% were present in our dataset, demonstrating strong concordance between our proteomic findings and previously published EV studies (Figure 2B). EV markers included CD9, Flotillin-1, Annexin A2, and Enolase 1, among others. The heatmap in Figure 2C illustrates the abundance of the top 15 EV markers in our dataset, with NG and P samples exhibiting the broadest range of EV markers compared to C, G and PG samples. Interestingly, hierarchical clustering revealed a separation in protein profiles, distinguishing non-pregnant samples from the others (Figure 2C).

We then examined each group individually. A Venn diagram comparing the five groups revealed that leukocyte immunoglobulin-like receptor subfamily B member 2 (LILRB2) was uniquely present in the co-infected women sample. Additionally, 34 proteins were exclusively identified in the P group, while 10 proteins were found only in the G group (Figure 3). Two proteins, a Z-dependent protease inhibitor (SERPINA10) and the C-reactive protein (CRP), were

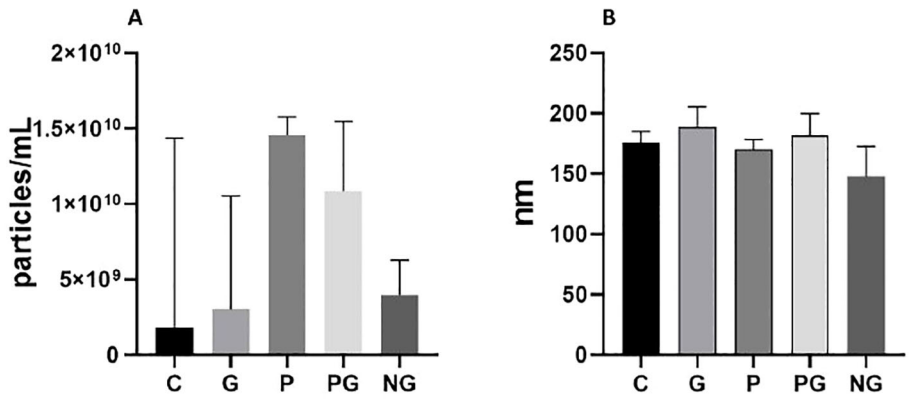

FIGURE 1
Comparison of concentration and size of EVs among the study groups. **(A)** Concentration of EVs in each group. Error bars show median and interquartile range. **(B)** Size of EVs in each study group. Error bars show median and interquartile range. Groups: C: pregnant women without infection. G: pregnant women with soil-transmitted helminths infection. P: Pregnant women with *Plasmodium* infection. PG: pregnant women coinfected by *Plasmodium* and soil-transmitted helminths. NG: Non-pregnant women. Pregnant women infected with *Plasmodium* showed the highest concentration of EVs, while uninfected non-pregnant women showed the lowest concentration **(A)**. Infected pregnant women showed EVs with a range of size more variable than non-pregnant women **(B)**.

present in all infected groups, corresponding to P, G, and PG groups. Furthermore, 8 proteins were common to both G and P, 7 were shared between G and PG, and 7 were found in both P and PG. In total, 69 human proteins were uniquely identified in the infected groups, encompassing *Plasmodium* infection, STH infection, and co-infection. Moreover, several proteins were detected only in healthy donor samples. Details on these proteins can be found in Supplementary Table 1.

To further explore the functional implications of the proteins only identified in the infected samples and not found in the control samples, as well as their combinations, we conducted a GO annotation and a KEGG pathway enrichment analysis. These analyses aimed to elucidate the biological processes, molecular functions, cellular components and pathways associated with the proteome dataset. Regarding enriched biological processes, we identified proteins associated with female pregnancy, heterophilic cell-cell adhesion via plasma membrane, cell adhesion molecules, proteolysis, blood coagulation and regulation of the immune response system, among others (Figures 4A–C). Moreover, the analysis revealed significant enrichment in cellular components related to extracellular exosomes, extracellular region, extracellular space, cell surface, and plasma membrane. This suggests a strong presence of proteins involved in extracellular communication through extracellular vesicles. The molecular function enrichment highlighted that many proteins in this dataset are involved in protein tyrosine kinase binding, serine-type endopeptidase activity and calcium ion binding. Finally, the two most prominent KEGG pathways identified were the complement and coagulation cascades and the renin-angiotensin system (Figure 4D). Details on detected proteins in patients with *Plasmodium* and/or STH infections are shown in Tables 3 and 4.

3.5 Identification of parasite proteins in plasma-derived EVs

Finally, the analysis of the data obtained from LC-MS with the Proteome Discoverer v2.5 software, resulted in the identification, with high confidence, of six proteins of *P. vivax* in the EVs from pregnant women infected only with malaria parasites (group P); 15 proteins of *T. trichiura*, and one protein of *N. americanus* (Tables 3 and 4) in the EVs from pregnant women infected only with STH (group G). Unexpectedly, parasite proteins were not identified in the group of coinfected pregnant women (group PG).

4 Discussion

The role of EVs as important intercellular communicators gives them increasing relevance as mediators of various scenarios within the pathophysiology of infectious diseases (Marcilla et al., 2014; Schorey et al., 2015), but there are many questions and challenges regarding the true scope of their functions in a variety of scenarios (van Niel et al., 2022). For example, in physiological processes such as pregnancy, in pathological states due to infections with invasive agents (Condrat et al., 2021) and in scenarios that combine the infectious process and a physiological condition. In relation to the latter, the little that has been studied has been especially focused on viral infections (Bayer et al., 2016; Condrat et al., 2021; Kaminski et al., 2019). Knowledge about the role of EVs in gestational parasitic infections, particularly due to *Plasmodium* and STH, is almost non-existent. In the case of malaria, most of this information has been obtained from indirect associations of circulating microparticles in human infections with disease severity, as well as from extrapolations from studies using EVs obtained from *in*

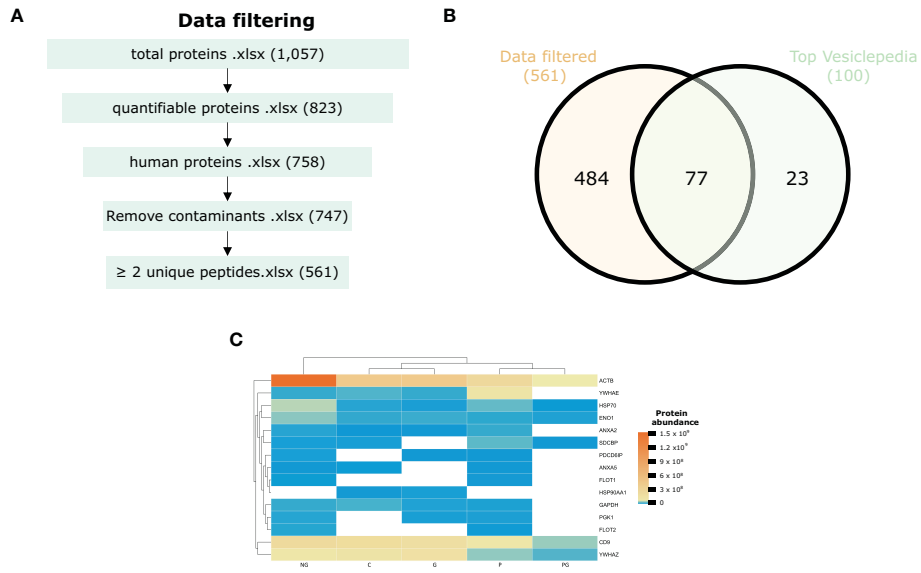

FIGURE 2
Proteomic profile of EVs. **(A)** Schematic workflow for quantitative proteomics and bioinformatic analysis. **(B)** Venn diagram of the number of unique proteins identified in EVs in the Vesiclepedia top 100 EV marker list. **(C)** Heatmap illustrating the top 15 enriched common EV proteins across the samples based on their protein intensity as determined from the proteome data. C, pregnant women without infection; G, pregnant women with STH infection; P, pregnant women with *Plasmodium* infection; PG, pregnant women with coinfection with *Plasmodium* and STH; NG, non-pregnant women.

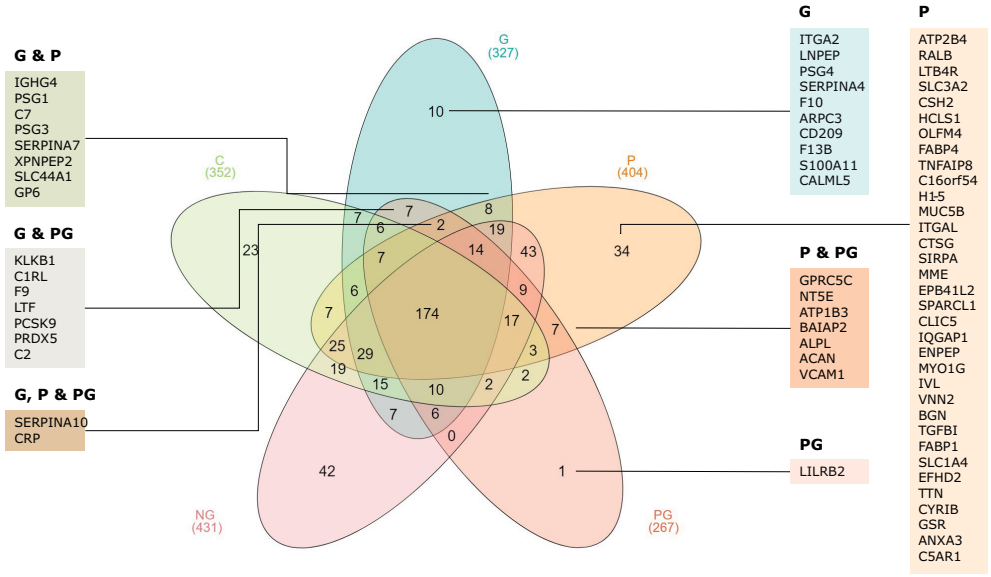

FIGURE 3
Venn diagram representing the overlap of detected proteins across the five samples. The diagram illustrates the shared and unique proteins identified in each group, with the corresponding gene IDs displayed. C, pregnant women without infection; G, pregnant women with STH infection; P, pregnant women with *Plasmodium* infection; PG, pregnant women with coinfection with *Plasmodium* and STH; NG, non-pregnant women.

vitro cultures or animal models (Campos et al., 2010; Khowawisetsut and Khunweeraphong, 2019; Nantakomol et al., 2011). Yet, circulating trophoblast microparticles have been study in the context of malaria and HIV infections, showing higher concentrations in HIV and identifying miR-517c as an over-expressed micro-RNA in mothers with placental malaria (Moro et al., 2016).

The few studies on soluble mediators in infections caused by *Plasmodium* and/or STH do not include pregnant women nor evaluate EVs (Bwanika et al., 2018; de Oliveira Menezes et al., 2018). In this study, we sought to obtain information on the role of EVs in the context of *Plasmodium* and/or STH during pregnancy and for this purpose, the isolation and characterization of the EVs of

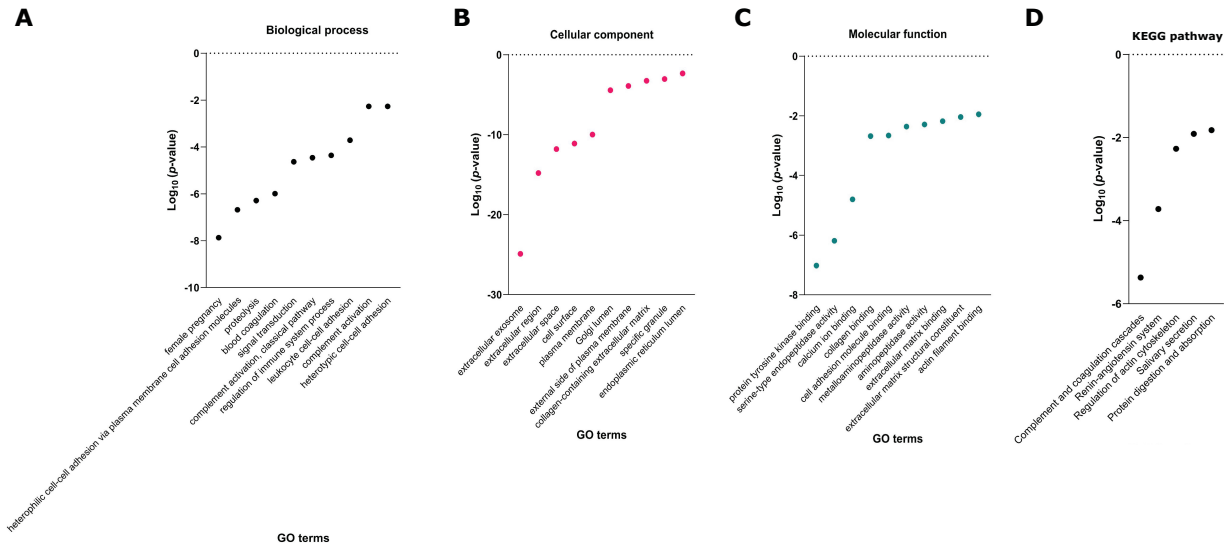

FIGURE 4
Gene Ontology (GO) annotation of **(A)** biological process, **(B)** cellular component and **(C)** molecular function, and **(D)** Kyoto Encyclopedia of Genes and Genomes (KEGG) pathway enrichment analyses of proteins exclusively detected in infected samples (P, G, PG, P&G, P&PG, G&PG, P&G&PG). C, pregnant women without infection; G, pregnant women with STH infection; P, pregnant women with *Plasmodium* infection; PG, pregnant women with coinfection with *Plasmodium* and STH; NG, non-pregnant women.

10.3389/fmala.2024.1484359

TABLE 3 Proteins of *Plasmodium* and soil-transmitted helminths identified in extracellular vesicles isolated from infected pregnant women.

UniProt Accession	Description	UP	Peptide sequence	Abundance
Plasmodium vivax proteins				
A5KCK3	Phist protein (Pf-fam-n) OS= Plasmodium vivax	9	[K].DDEGNVIRPAGK.[H] [R].AELQEQMTEEELNSK.[I] [K].SFDDEYHGR.[G] [R].HDDQFFDEGR.[F] [R].SEQIAAMNYEEQFHQGPR.[G] [K].GDDSSVTPSPENPDDPNNPPSTTE TPGNSDGEHK.[D] [K].DNVIRPDQPAPVKPDGDDTGK.[G] [R].WQEEEDMYNPR.[M] [K].ERGDFQDFYAFVSK.[G]	1709161.83
A5K8G8	Membrane associated histidine-rich protein 2 OS=Plasmodium vivax	2	[K].SDDEDSYNYDDSEEK.[E] [K].FYQTVVHR.[Y]	6282779.5
A5K904	Osmiophilic body protein G377 OS=Plasmodium vivax	2	[K].LAEFIDSR.[A] [K].EAQEENTADENHADVYAR.[E]	4537682.5
A5K1L4	Pv-fam-d protein OS Plasmodium vivax	2	[R].YVSPGNNFNK.[E] [R].SEFGSQGEQSQFVNGDNTNEQR.[D]	4308140.5
A5K8G9	ShKT domain-containing protein OS=Plasmodium vivax	2	[K].KAEAIVDAGAQALNGLK.[N] [K].TLDLYFEK.[K]	12065028
A5KAV2	Merozoite suface protein 3 beta (MSP3b) OS=Plasmodium vivax	1	[R].IEAEEAEK.[E]	2057069.4
Trichiuris trichiura and *Necator americanus* proteins				
A0A077ZAW5	Mitocondrial chaperonin hsp60 OS=Trichiuris trichiura	14	[K].AIAQVGTISANSDETVGK.[L] [K].ANDAAGDGTTTATVLAQAIITEGLK.[A] [K].AMLQDIATLTGGTVISEEIGMELEK.[A] [K].AVAAGMNPMDLK.[R] [K].DTTTIIDGVGEEAAIQGR.[V] [K].VGAATEVEMK.[E] [K].LIAEAMDK.[V] [K].ATLEDLGQAK.[R] [K].LAGGVAVIK.[V] [R].GYLSPYFINKPETGAVELESPFILLADK.[K] [K].DGVSVAR.[E] [K].SFGAPTITK.[D] [R].GVNVLADAVK.[V] [K].FENMGAQMVK.[E]	1392133955
A0A077ZHF8	UPF0066 and Lipoprotein 9 domain containing protein OS=Trichiuris trichiura	5	[R].SLDDAQIALAVINTTYASQIGLTPAK.[D] [K].VGVIVGAEQQVAEVAQK.[V] [K].IVELEAPQLPR.[S] [K].DGIFVEDK.[E] [K].YGLDVELVTFNDYVLPNEALSK.[G]	167457848
A0A077ZIV8	Ribosomal L10 domain containing protein OS=Trichiuris trichiura	3	[R].LATLPTYEEAIAR.[L] [K].GALSAVVADSR.[G] [K].AAAFEGELIPASQIDR.[L]	12646973.5
A0A077ZGP0	Serine-type D-AlaD-Ala carboxypeptidase OS=Trichiuris trichiura	3	[K].NQVVGTINFQLDGK.[T] [R].FFETVNPLK.[V] [R].DMALIGQALIR.[D]	8252966
A0A077ZFP3	UPF and LppC and SIS 2 and BON domain containing ing protein OS=Trichiuris trichiura	2	[R].INVTAYQGK.[V] [R].TIQQGFEAAK.[N]	21668530
A0A077ZMJ5	Phosphoglycerate kinase OS=Trichiuris trichiura	3	[K].KDDETLSK.[K] [K].SLYEADLVDEAK.[R] [R].ASLPTIELALK.[Q]	7747544
A0A077ZM27	Multifunctional fusion protein OS=Trichiuris trichiura	2	[K].TEFDVILK.[A] [K].DLVESAPAALK.[E]	116045568
A0A077ZH99	Elongation factor Tu OS=Trichiuris trichiura	2	[K].VGEEVEIVGIK.[E] [K].ILELAGFLDSYIPEPER.[A]	8466110

(Continued)

TABLE 3 Continued

UniProt Accession	Description	UP	Peptide sequence	Abundance
Trichiuris trichiura and *Necator americanus* proteins				
A0A077ZM69	RecA and CinA domain containing protein	2	[R].SGAVDVIVVDSVAALTPK.[A] [K].AEIEGEIGDSHMGLAAR.[M]	44965836
A0A077Z5U3	ATP-synt B domain containing protein OS=Trichiuris trichiura	2	[K].EIADGLASAER.[A] [K].QVAILAVAGAEK.[I]	3812519.6
A0A077ZG46	Glucose fructose oxidoreductase OS=Trichiuris trichiura	1	[K].AVVEAIK.[L]	15050138
A0A077ZKG5	OEP domain containing protein OS=Trichiuris trichiura	1	[K].QAQYNFVGASEQLESAHR.[S]	2291416
W2TXM2	LigA OS=Necator americanus	1	[R].VERDGIEVEEAVGAVR.[I]	18904494
A0A077ZBR7	Aspartate ammonia-lyase OS=Trichiuris trichiura	1	[K].AVEFQDILK.[M]	5526022
A0A077ZHD8	PPQ 2 domain containing protein OS=Trichiuris trichiura	1	[R].ISQATGSTEIDR.[L]	62155152
A0A077ZJ70	Ribosomal protein OS=Trichiuris trichiura	1	[K].VGTVTPNVAEAVK.[N]	2891247.2

TABLE 4 Characteristics of the parasite proteins identified in extracellularvesicles isolated from infected pregnant women.

UniProt Accession	Protein features	Subcellular location	Cellular Component	Biological process	Molecular function
Plasmodium vivax proteins					
A5KCK3	Transmembrane domain	Membrane	Membrane	Uncharacterized	Uncharacterized
A5K8G8	Transmembrane domain	Membrane	Membrane	Uncharacterized	Uncharacterized
A5K904	Signal peptide domain*	Uncharacterized	Uncharacterized	Uncharacterized	Uncharacterized
A5K1L4	Transmembrane domain	Membrane	Membrane	Uncharacterized	Uncharacterized
A5K8G9	Uncharacterized	Uncharacterized	Uncharacterized	Uncharacterized	Uncharacterized
A5KAV2	Signal peptide domain*	Uncharacterized	Uncharacterized	Uncharacterized	Uncharacterized
Trichiuris trichiura and *Necator americanus* proteins					
A0A077ZAW5	Mitochondrial chaperonin domain	GroEL-GroES complex	GroEL-GroES complex	Refolding protein	ATP-dependent protein folding chaperone
A0A077ZHF8	Signal peptide domain*	Membrane	Membrane	Intracellular signal transduction	Uncharacterized
A0A077ZIV8	Universal ribosomal protein uL10 family	Cytosolic large ribosomal subunit	Cytosolic large ribosomal subunit	Translation	Structural constituent of ribosome
A0A077ZGP0	Signal peptide domain*	Uncharacterized	Uncharacterized	Proteolysis	Serine-type D-Ala-D-Ala carboxypeptidase activity
A0A077ZFP3	Signal peptide domain*	Uncharacterized	Uncharacterized	DNA repair	Carbohydrate derivative binding
A0A077ZMJ5	Enzymatic domain	Cytoplasm	Cytoplasm	Glycolytic process	Phosphoglycerate kinase activity
A0A077ZM27	Enzymatic domain	Nuclear lumen	DNA-directed RNA polymerase complex	DNA-templated transcription	DNA-directed 5'-3' RNA polymerase activity
A0A077ZH99	Enzymatic domain	Cytosol	Cytosol	Translation	Translation elongation factor activity
A0A077ZM69	Enzymatic domain	Cytosol	Cytosol	DNA repair	ATP-dependent DNA damage sensor activity

(Continued)

TABLE 4 Continued

UniProt Accession	Protein features	Subcellular location	Cellular Component	Biological process	Molecular function
Trichiuris trichiura and *Necator americanus* proteins					
A0A077Z5U3	Enzymatic domain	Membrane	Plasma membrane	Proton motive force-driven ATP synthesis	Proton-transporting ATPase activity, rotational mechanism
A0A077ZG46	Enzymatic domain	Uncharacterized	Uncharacterized	Uncharacterized	Nucleotide binding
A0A077ZKG5	Signal peptide domain*	Outer membrane	Outer membrane	Efflux transmembrane transporter activity	Porin activity
W2TXM2	Uncharacterized	Uncharacterized	Uncharacterized	Uncharacterized	Uncharacterized
A0A077ZBR7	Enzymatic domain	Uncharacterized	Uncharacterized	Aspartate metabolic process	Aspartate ammonia-lyase activity
A0A077ZHD8	Uncharacterized	Uncharacterized	Uncharacterized	Uncharacterized	Uncharacterized
A0A77ZJ70	Uncharacterized	Uncharacterized	Uncharacterized	Uncharacterized	Uncharacterized

*Signal peptide domain: Signal peptides are found in proteins that are targeted to the endoplasmic reticulum and eventually destined to be either secreted/extracellular/periplasmic/etc., retained in the lumen of the endoplasmic reticulum, of the lysosome or of any other organelle along the secretory pathway or to be I single-pass membrane proteins.

pregnant women with *Plasmodium* and/or STH infection residing in Colombian areas co-endemic for those parasites, was carried out.

The isolation and purification of circulating EVs from plasma was done by SEC, a technique already proven to be robust for isolating exosomes free from soluble plasma proteins (de Menezes-Neto et al., 2015). In this work, we used the tetraspanin CD9 to identify EV-rich fractions, the effectiveness of the technique for isolating and enriching EVs from plasma samples, with very low amount of soluble plasma proteins not associated with EVs, most of which correspond to exosomes based on their size and expression of CD9, was once again demonstrated (de Menezes-Neto et al., 2015; Díaz-Varela et al., 2018; Gualdrón-López et al., 2018; Toda et al., 2020).

Our results suggest that the infectious state may have the ability to modulate the production of EVs according to their relative abundance and size, as we found that the highest amount of EVs in the control groups C and NG were concentrated in the size range of 50 to 300 nm, while in the infection groups, the range of sizes is much more variable (100 to 700 nm) (Figure 1, Supplementary Figure 2). Additionally, our results suggest that monoinfection by *Plasmodium* or STH may favor a higher production of EVs, as we found higher expression of CD9 in monoinfected pregnant women (Supplementary Figure 2). Furthermore, it appears that the absence of pregnancy and plasmodial infection promote the maximum amount of proteins in EVs, while pregnancy and simultaneous Plasmodium-STH coinfection lead to the minimum amount.

Other studies have demonstrated an increase in the abundance of circulating EVs in patients compared to healthy donors during natural *Plasmodium* infections (Campos et al., 2010; Nantakomol et al., 2011; Toda et al., 2020). However, although in our study there is an increase in the concentration of particles in the groups with infections, including pregnant women with malaria, this difference does not have statistical significance (Figure 1), likely due to the limited sample size we had. It is thus necessary to validate the results in future studies with larger sample sizes to provide further epidemiological support to the findings.

In this study, we demonstrated the presence of parasite proteins in EVs from pregnant women infected with *P. vivax* (6 proteins) or STH (16 proteins) using SEC as a method for isolation and enrichment of plasma-derived EVs. Although SEC proved to be a robust method for isolating plasma-derived EVs, other methods such as immunocapture may be advantageous for achieving higher enrichments of parasite-derived EVs; however, immunocapturing only have been used for enrichment of EVs from *P. vivax* via CD71 (Aparici-Herraiz et al., 2022), but for STH is challenging due to the scarcity of antibodies suitable for helminths (Stam et al., 2021).

When looking into the human protein signatures found in the EVs profiled in this study, we were able to observe a diverse set of molecular mechanisms crucial for various physiological and pathological states. These functions involve immune regulation, cellular signaling, enzymatic activity and structural roles, highlighting the complexity of biological systems. For instance, LILRB2, a protein exclusively found in the PG group, is a molecule well known to acts as a receptor for class I MHC antigens and is involved in down-regulating immune responses, critical for maintaining maternal-fetal tolerance (Gregori et al., 2010; Lepin et al., 2000; Shiroishi et al., 2003, 2006). Also, enzymes like RALB, which is a GTPase involved in diverse cellular processes, including cell migration and apoptosis suppression (Cascone et al., 2008; Falsetti et al., 2007) or receptors like the LTB4R functions as a receptor for leukotriene B4, playing a role in inflammation and immune responses (He et al., 2020; Miyabe et al., 2017) or the CD209 functions as a pathogen-recognition receptor on dendritic cells, crucial for initiating immune responses by presenting antigens to T-cells (Khoo et al., 2008; Mason and Tarr, 2015) were detected in P and G groups exclusively (Figure 3). This diversity illustrates the range of cellular processes these proteins influence, from immune modulation to intracellular signaling and structural integrity.

Shared among infected groups (P, G and PG), proteins like the F9, essential in the intrinsic pathway of blood coagulation by converting factor X to its active form (Perez Botero et al., 2018), or

KLKB1 which plays a role in blood coagulation by activating factor XII and releasing bradykinin (Moellmer et al., 2024), highlights the importance of blood coagulation processes in the studied groups. Also, complement activation, as showed by the detection of C2 and C7 proteins, involved in immune defense through classical pathways and membrane attack complex formation were detected. From the two proteins shared among the three infected groups (Figure 3) C-reactive protein has been detected, which is an acute phase protein ubiquitously elevated in any inflammatory response (Wilairatana et al., 2021), thus compromising its use as a parasite infection/disease specific biomarker.

We highlight that this is the first study that identifies, through mass spectrometry associated with liquid chromatography, the presence of *Plasmodium* and STH proteins in EVs of pregnant women. Among the most important findings is the identification, with high confidence and abundance, of the Plasmodium helical interspersed subtelomeric (PHIST) protein of *P. vivax* (PVX_093680) also known as PHIST Caveola-vesicle complexes (CVC)-81$_{95}$ (Warncke et al., 2016), in the group of pregnant women with malaria; though the presence of this family of proteins has already been demonstrated in EVs from patients infected by *P. vivax* but not pregnant (Aparici-Herraiz et al., 2022; Toda et al., 2020). These PHIST proteins are part of a family of approximately 89 members, which are exported by *Plasmodium* during its asexual cycle and are thought to be involved in host cell remodeling during infection. Although their exact function is not yet known, these proteins have been mostly characterized by *P. falciparum* and there is not much information about their expression in *P. vivax* (Warncke et al., 2016). Interestingly, PHIST CVC-81$_{95}$ is the best characterized non-*P. falciparum* PHIST protein and belongs to *P. vivax*. Although its function and structure are not yet known exactly, it has been found in caveolae-vesicle complexes (Akinyi et al., 2012), which are parasite-induced clefts in the cell membranes of erythrocytes infected with *P. vivax*, and in peripheral blood of infected individuals (Acharya et al., 2009). Furthermore, a study found antibody response against PHIST CVC-81$_{95}$ in a high percentage of serum samples from patients (Lu et al., 2014), suggesting a possible role of this protein in the immune response during *P. vivax* infection. Our findings demonstrate the presence of this protein additionally in EVs of pregnant women infected with *P. vivax*, which reinforces the theory of a possible role of this protein as a possible biomarker or inducer of the immune response during the parasite-host interaction. However, more functional analyzes are needed to fully understand the role of this PHIST protein in *P. vivax* CVC, particularly in pregnant women.

Another protein associated with EVs from pregnant women infected with *Plasmodium* found in our study was the merozoite surface protein 3β from *P. vivax*-PvMSP-3β (PVX_097680). Although there is little literature about the functionality of this protein, its gene is highly polymorphic and has been used mainly to determine the genetic diversity of strains in *P. vivax* in epidemiological studies (Li et al., 2022; Rayner et al., 2004). Particularly, only one study demonstrated the immunogenic capacity of the recombinant antigen of the PvMSP-3β protein in mice, in which high titers of antibodies capable of recognizing infected erythrocytes extracted from patients with *P. vivax* malaria were produced, proposing a possible use of this recombinant antigen as a candidate for vaccine production (Bitencourt et al., 2013). In this study, we found this protein associated with EVs in infected pregnant women, which leads us to suggest, considering the immunogenic capacity previously demonstrated for PvMSP-3β, that these purified EVs could be used in the future as possible vaccine candidates against *P. vivax* infection.

It is important to mention that an exhaustive search was carried out on the functionality of the other proteins identified from *P. vivax* in the proteomic analysis, using databases such as UniProt (https://www.uniprot.org/), NCBI (https://www.ncbi.nlm.nih.gov/), and STRING (https://string-db.org/), but it was not obtained any satisfactory result because those protein have not yet been characterized. Something similar occurred for the proteins identified from *T. trichiura* and *N. amaricanus*, for which although their participation in metabolic processes and flow of genetic information of the parasite can be deduced, they are still not sufficiently characterized and their functionality in the parasite host interaction has not been determined. However, the fact of having found so many of these proteins associated with the EVs of pregnant women infected with STH encourages us to suggest a possible role of these proteins in the modulation of the immune response during chronic infection by these parasites. Many future functional studies are necessary to help determine the role of these EV-associated proteins during infection in pregnant women.

Altogether, our results showed the presence of *Plasmodium* and STH proteins in the EVs of pregnant women, which opens a challenging field of study to elucidate the true role of EVs in the immunomodulation and pathophysiology of these infections during pregnancy. New functional studies are required that evaluate in greater depth the effects of EVs isolated from coinfected or monoinfected pregnant women, both at the level of the immune response and in the pathophysiology of these infections, to obtain more understanding of the consequences caused by the presence of these agents during pregnancy, as has been proposed (Buzas, 2022).

In conclusion, this is the first study that identifies *Plasmodium* proteins and proteins from intestinal worms infecting humans that are transmitted through contaminated soil in EVs isolated from pregnant women. The set of results indicates that pregnancy and infections by *Plasmodium* and/or STH modulate the production of EVs in Colombian areas co-endemic for those parasites. The identification of such proteins from neglected tropical parasites accounting for a major burden of disease worldwide open the possibilities of studying their physiological role during infections as well as exploring them for antigen discovery, vaccine development and biomarker discovery.

Data availability statement

The original contributions presented in the study are publicly available. The mass spectrometry proteomics data have been deposited to the ProteomeXchange Consortium (identifier PXD055557) via the PRIDE partner repository.

Ethics statement

The studies involving humans were approved by Ethics Committee of the Medical Research Institute of the University of Antioquia. The studies were conducted in accordance with the local legislation and institutional requirements. Written informed consent for participation in this study was provided by the participants' legal guardians/next of kin.

Author contributions

JM-M: Conceptualization, Investigation, Writing – original draft. AA-H: Formal analysis, Writing – review & editing. BB-C: Formal analysis, Writing – review & editing. CF-B: Supervision, Writing – review & editing. HP: Conceptualization, Supervision, Writing – review & editing. JC-F: Conceptualization, Supervision, Writing – review & editing. EA-F: Conceptualization, Project administration, Supervision, Writing – review & editing.

Funding

The author(s) declare financial support was received for the research, authorship, and/or publication of this article. Minciencias-Colombia project code 111584467512, Contract 850-2022. Universidad de Antioquia. Fundación Universitaria San Martín. CF-B and HP acknowledge support from the grant CEX2023-0001290-S funded by MCIN/AEI/10.13039/501100011033, and support from the Generalitat de Catalunya through the CERCA Program. CF-B is also part of the CIBER-Consorcio Centro de Investigación Biomédica en Red (CB 2021), Instituto de Salud Carlos III, Ministerio de Ciencia e Innovación, and Unión Europea–NextGenerationEU. This research is part of the ISGlobal's Program on the Molecular Mechanisms of Malaria which is partially supported by the Fundación Ramón Areces.

Acknowledgments

To Eva Borrás and Eduard Sabidó for helpful discussions on the LC-MS data. To Paula Crego and Marc Nicolau for assistance in isolation and characterization of plasma-derived EVs. The CRG/UPF Proteomics Unit is part of the Spanish Infrastructure for Omics Technologies (ICTS OmicsTech), and it is supported by "Secretaria d'Universitats i Recerca del Departament d'Economia i Coneixement de la Generalitat de Catalunya" (2017SGR595).

Conflict of interest

The authors declare that the research was conducted in the absence of any commercial or financial relationships that could be construed as a potential conflict of interest.

Publisher's note

Supplementary material

The Supplementary Material for this article can be found online at: https://www.frontiersin.org/articles/10.3389/fmala.2024.1484359/full#supplementary-material

SUPPLEMENTARY FIGURE 1
Flowchart of the workflow for the isolation and phenotypic characterization of extracellular vesicles.

SUPPLEMENTARY FIGURE 2
(A) Comparison of median fluorescence intensity (MFI) for CD9 among the study groups. **(B)** Representative graph of the nanoparticle tracking analysis (NTA) per study group. C, pregnant women without infection; G, pregnant women with STH infection; P, pregnant women with *Plasmodium* infection; PG, pregnant women with coinfection with *Plasmodium* and STH; NG, non-pregnant women.

SUPPLEMENTARY FIGURE 3
Proteomic Profile of EV isolated by SEC from plasma samples of the five study groups. **(A, B)** Distribution of numbers of quantified **(A)** proteins and **(B)** peptides in the samples. **(C)** Distribution of peptide numbers of quantified proteins. C, pregnant women without infection; G, pregnant women with STH infection; P, pregnant women with *Plasmodium* infection; PG, pregnant women with coinfection with *Plasmodium* and STH; NG, non-pregnant women.

References

Acharya, P., Pallavi, R., Chandran, S., Chakravarti, H., Middha, S., Acharya, J., et al. (2009). A glimpse into the clinical proteome of human malaria parasites Plasmodium falciparum and Plasmodium vivax. *Proteomics Clin. Appl.* 3, 1314–1325. doi: 10.1002/PRCA.200900090

Akinyi, S., Hanssen, E., Meyer, E. V. S., Jiang, J., Korir, C. C., Singh, B., et al. (2012). A 95 kDa protein of Plasmodium vivax and P. cynomolgi visualized by 3-D tomography in the caveola-vesicle complexes (Schüffner's dots) of infected erythrocytes is a member of the PHIST family. *Mol. Microbiol.* 84, 816. doi: 10.1111/J.1365-2958.2012.08060.X

Álvarez-Larrotta, C., Agudelo, O. M., Duque, Y., Gavina, K., Yanow, S. K., Maestre, A., et al. (2019). Submicroscopic Plasmodium infection during pregnancy is associated with reduced antibody levels to tetanus toxoid. *Clin. Exp. Immunol.* 195, 96–108. doi: 10.1111/CEI.13213

Alvarez-Larrotta, C., Arango, E. M., and Carmona-Fonseca, J. (2018). Negative immunomodulation by parasitic infections in the human response to vaccines. *J. Infect. Dev. Ctries* 12, 812–823. doi: 10.3855/JIDC.10337

Aparici-Herraiz, I., Gualdrón-López, M., Castro-Cavadía, C. J., Carmona-Fonseca, J., Yasnot, M. F., Fernandez-Becerra, C., et al. (2022). Antigen discovery in circulating extracellular vesicles from plasmodium vivax patients. *Front. Cell Infect. Microbiol.* 11. doi: 10.3389/fcimb.2021.811390

Arango, E. M., Samuel, R., Agudelo, O. M., Carmona-Fonseca, J., Maestre, A., and Yanow, S. K. (2013). Molecular detection of malaria at delivery reveals a high frequency of submicroscopic infections and associated placental damage in pregnant women from northwest Colombia. *Am. J. Trop. Med. Hygiene* 89, 178–183. doi: 10.4269/AJTMH.12-0669/-/DC6/SD6.PDF

Banco Interamericano de Desarrollo, Organización Panamericana de la Salud and Instituto de Vacunas Sabin (2011). *Un Llamado a la Acción: Hacer frente a helmintos transmitidos por el suelo en América Latina y el Caribe*. Available online at: https://www.paho.org/es/documentos/llamado-accion-hacer-frente-helmintos-transmitidos-por-contacto-con-suelo-latino-0 (Accessed August 19, 2024).

Barreto, R. E., Narváez, J., Sepúlveda, N. A., Velásquez, F. C., Díaz, S. C., López, M. C., et al. (2017). Combination of five diagnostic tests to estimate the prevalence of hookworm infection among school-aged children from a rural area of Colombia. *Acta Trop.* 173, 160–170. doi: 10.1016/J.ACTATROPICA.2017.05.028

Basuni, M., Muhi, J., Othman, N., Verweij, J. J., Ahmad, M., Miswan, N., et al. (2011). A pentaplex real-time polymerase chain reaction assay for detection of four species of soil-transmitted helminths. *Am. J. Trop. Med. Hyg* 84, 338. doi: 10.4269/AJTMH.2011.10-0499

Bayer, A., Lennemann, N. J., Ouyang, Y., Bramley, J. C., Morosky, S., Marques, E. T. D. A., et al. (2016). Type III interferons produced by human placental trophoblasts confer protection against zika virus infection. *Cell Host Microbe* 19, 705–712. doi: 10.1016/J.CHOM.2016.03.008

Bitencourt, A. R., Vicentin, E. C., Jimenez, M. C., Ricci, R., Leite, J. A., Costa, F. T., et al. (2013). Antigenicity and immunogenicity of plasmodium vivax merozoite surface protein-3. *PLoS One* 8, e56061. doi: 10.1371/JOURNAL.PONE.0056061

Blackwell, A. D. (2016). Helminth infection during pregnancy: insights from evolutionary ecology. *Int. J. Womens Health* 8, 651. doi: 10.2147/IJWH.S103529

Buck, A. H., Coakley, G., Simbari, F., McSorley, H. J., Quintana, J. F., Le Bihan, T., et al. (2014). Exosomes secreted by nematode parasites transfer small RNAs to mammalian cells and modulate innate immunity. *Nat. Commun.* 5, 5488. doi: 10.1038/NCOMMS6488

Buzas, E. I. (2022). The roles of extracellular vesicles in the immune system. *Nat. Rev. Immunol.* 23, 236–250. doi: 10.1038/s41577-022-00763-8

Bwanika, R., Kato, C. D., Welishe, J., and Mwandah, D. C. (2018). Cytokine profiles among patients co-infected with Plasmodium falciparum malaria and soil borne helminths attending Kampala International University Teaching Hospital, in Uganda. *Allergy Asthma Clin. Immunol.* 14, 10. doi: 10.1186/S13223-018-0235-Z

Campos, F. M., Franklin, B. S., Teixeira-Carvalho, A., Filho, A. L., De Paula, S. C., Fontes, C. J., et al. (2010). Augmented plasma microparticles during acute Plasmodium vivax infection. *Malar J.* 9, 327. doi: 10.1186/1475-2875-9-327

Carmona-Fonseca, J. (2020). The Epidemiology of Malaria in Colombia: a heretical view. *Soc Med.* 20 (2), 75–87. Available at: https://www.socialmedicine.info/index.php/socialmedicine/article/view/1237.

Cascone, I., Selimoglu, R., Ozdemir, C., Del Nery, E., Yeaman, C., White, M., et al. (2008). Distinct roles of RalA and RalB in the progression of cytokinesis are supported by distinct RalGEFs. *EMBO J.* 27, 2375–2387. doi: 10.1038/EMBOJ.2008.166

Chen, C., Wu, Y., Li, J., Wang, X., Zeng, Z., Xu, J., et al. (2023). TBtools-II: A "one for all, all for one" bioinformatics platform for biological big-data mining. *Mol. Plant* 16, 1733–1742. doi: 10.1016/J.MOLP.2023.09.010

Chitti, S. V., Gummadi, S., Kang, T., Shahi, S., Marzan, A. L., Nedeva, C., et al. (2024). Vesiclepedia 2024: an extracellular vesicles and extracellular particles repository. *Nucleic Acids Res.* 52, D1694. doi: 10.1093/NAR/GKAD1007

Condrat, C. E., Varlas, V. N., Duică, F., Antoniadis, P., Danila, C. A., Cretoiu, D., et al. (2021). Pregnancy-related extracellular vesicles revisited. *Int. J. Mol. Sci.* 22, 3904. doi: 10.3390/IJMS22083904

Crompton, P. D., Moebius, J., Portugal, S., Waisberg, M., Hart, G., Garver, L. S., et al. (2014). Malaria immunity in man and mosquito: insights into unsolved mysteries of a deadly infectious disease. *Annu. Rev. Immunol.* 32, 157–187. doi: 10.1146/ANNUREV-IMMUNOL-032713-120220

Debs, S., Cohen, A., Hosseini-Beheshti, E., Chimini, G., Hunt, N. H., and Grau, G. E. R. (2019). Interplay of extracellular vesicles and other players in cerebral malaria pathogenesis. *Biochim. Biophys. Acta Gen. Subj* 1863, 325–331. doi: 10.1016/J.BBAGEN.2018.10.012

Dekel, E., Yaffe, D., Rosenhek-Goldian, I., Ben-Nissan, G., Ofir-Birin, Y., Morandi, M. I., et al. (2021). 20S proteasomes secreted by the malaria parasite promote its growth. *Nat. Commun.* 12, 1172. doi: 10.1038/s41467-021-21344-8

de Menezes-Neto, A., Sáez, M. J., Lozano-Ramos, I., Segui-Barber, J., Martin-Jaular, L., Ullate, J. M. E., et al. (2015). Size-exclusion chromatography as a stand-alone methodology identifies novel markers in mass spectrometry analyses of plasma-derived vesicles from healthy individuals. *J. Extracell Vesicles* 4, 27378. doi: 10.3402/JEV.V4.27378

de Oliveira Menezes, R. A., Mendonça Gomes, M., do, S., Mendes, A. M., D'Almeida Couto, Á.A.R., Nacher, M., et al. (2018). Enteroparasite and vivax malaria co-infection on the Brazil-French Guiana border: Epidemiological, haematological and immunological aspects. *PLoS One* 13, e0189958. doi: 10.1371/JOURNAL.PONE.0189958

Díaz-Varela, M., de Menezes-Neto, A., Perez-Zsolt, D., Gámez-Valero, A., Seguí-Barber, J., Izquierdo-Useros, N., et al. (2018). Proteomics study of human cord blood reticulocyte-derived exosomes. *Sci. Rep.* 8, 1 8, 1–1 8,11. doi: 10.1038/s41598-018-32386-2

Falsetti, S. C., Wang, D., Peng, H., Carrico, D., Cox, A. D., Der, C. J., et al. (2007). Geranylgeranyltransferase I inhibitors target RalB to inhibit anchorage-dependent growth and induce apoptosis and RalA to inhibit anchorage-independent growth. *Mol. Cell Biol.* 27, 8003–8014. doi: 10.1128/MCB.00057-07

Freitas do Rosario, A. P., and Langhorne, J. (2012). T cell-derived IL-10 and its impact on the regulation of host responses during malaria. *Int. J. Parasitol.* 42, 549–555. doi: 10.1016/J.IJPARA.2012.03.010

Fuhrmann, G., Neuer, A. L., and Herrmann, I. K. (2017). Extracellular vesicles - A promising avenue for the detection and treatment of infectious diseases? *Eur. J. Pharm. Biopharm* 118, 56–61. doi: 10.1016/J.EJPB.2017.04.005

Gavina, K., Arango, E., Larrotta, C. A., Maestre, A., and Yanow, S. K. (2017). A sensitive species-specific reverse transcription real-time PCR method for detection of Plasmodium falciparum and Plasmodium vivax. *Parasite Epidemiol. Control* 2, 70. doi: 10.1016/J.PAREPI.2017.04.001

Gazzinelli-Guimaraes, P. H., and Nutman, T. B. (2018). Helminth parasites and immune regulation. *F1000Res* 7, 1685. doi: 10.12688/F1000RESEARCH.15596.1

Gregori, S., Tomasoni, D., Pacciani, V., Scirpoli, M., Battaglia, M., Magnani, C. F., et al. (2010). Differentiation of type 1 T regulatory cells (Tr1) by tolerogenic DC-10 requires the IL-10-dependent ILT4/HLA-G pathway. *Blood* 116, 935–944. doi: 10.1182/BLOOD-2009-07-234872

Gualdrón-López, M., Flannery, E. L., Kangwanrangsan, N., Chuenchob, V., Fernandez-Orth, D., Segui-Barber, J., et al. (2018). Characterization of Plasmodium vivax Proteins in plasma-derived exosomes from Malaria-infected liver-chimeric humanized mice. *Front. Microbiol.* 9. doi: 10.3389/FMICB.2018.01271/BIBTEX

He, R., Chen, Y., and Cai, Q. (2020). The role of the LTB4-BLT1 axis in health and disease. *Pharmacol. Res.* 158, 104857. doi: 10.1016/J.PHRS.2020.104857

Heberle, H., Meirelles, V. G., da Silva, F. R., Telles, G. P., and Minghim, R. (2015). InteractiVenn: a web-based tool for the analysis of sets through Venn diagrams. *BMC Bioinf.* 16, 169. doi: 10.1186/S12859-015-0611-3

Honkpéhèdji, Y. J., Adegbite, B. R., Zinsou, J. F., Dejon-Agobé, J. C., Edoa, J. R., Zoleko Manego, R., et al. (2021). Association of low birth weight and polyparasitic infection during pregnancy in Lambaréné, Gabon. *Trop. Med. Int. Health* 26, 973–981. doi: 10.1111/tmi.13591

Huang, D. W., Sherman, B. T., and Lempicki, R. A. (2008). Systematic and integrative analysis of large gene lists using DAVID bioinformatics resources. *Nat. Protoc.* 4, 44–57. doi: 10.1038/nprot.2008.211

Huang, D. W., Sherman, B. T., and Lempicki, R. A. (2009). Bioinformatics enrichment tools: paths toward the comprehensive functional analysis of large gene lists. *Nucleic Acids Res.* 37, 1–13. doi: 10.1093/NAR/GKN923

Jamieson, D. J., Theiler, R. N., and Rasmussen, S. A. (2006). Emerging infections and pregnancy. *Emerg. Infect. Dis.* 12, 1638–1643. doi: 10.3201/EID1211.060152

Jeppesen, D. K., Zhang, Q., Franklin, J. L., and Coffey, R. J. (2023). Extracellular vesicles and nanoparticles: emerging complexities. *Trends Cell Biol.* 33, 667–681. doi: 10.1016/j.tcb.2023.01.002

Kalra, H., Simpson, R. J., Ji, H., Aikawa, E., Altevogt, P., Askenase, P., et al. (2012). Vesiclepedia: a compendium for extracellular vesicles with continuous community annotation. *PLoS Biol.* 10, e1001450. doi: 10.1371/JOURNAL.PBIO.1001450

Kaminski, V., de, L., Ellwanger, J. H., and Chies, J. A. B. (2019). Extracellular vesicles in host-pathogen interactions and immune regulation - exosomes as emerging actors in the immunological theater of pregnancy. *Heliyon* 5, e02355. doi: 10.1016/J.HELIYON.2019.E02355

Khoo, U. S., Chan, K. Y. K., Chan, V. S. F., and Lin, C. L. S. (2008). DC-SIGN and L-SIGN: the SIGNs for infection. *J. Mol. Med. (Berl)* 86, 861–874. doi: 10.1007/S00109-008-0350-2

Khowawisetsut, L., and Khunweeraphong, N. (2019). Extracellular vesicles in malaria infection. *Siriraj Med. J.* 71, 89–94. doi: 10.33192/SMJ.2019.14

Lepin, E. J. M., Bastin, J. M., Allan, D. S. J., Roncador, G., Braud, V. M., Mason, D. Y., et al. (2000). Functional characterization of HLA-F and binding of HLA-F tetramers to ILT2 and ILT4 receptors. *Eur J Immunol.* 30 (12), 3552–61. doi: 10.1002/1521-4141(200012)30:12

Li, X., Bai, Y., Wu, Y., Zeng, W., Xiang, Z., Zhao, H., et al. (2022). PvMSP-3α and PvMSP-3β genotyping reveals higher genetic diversity in Plasmodium vivax parasites from migrant workers than residents at the China-Myanmar border. *Infect. Genet. Evol.* 106, 105387. doi: 10.1016/J.MEEGID.2022.105387

Lu, F., Li, J., Wang, B., Cheng, Y., Kong, D. H., Cui, L., et al. (2014). Profiling the humoral immune responses to Plasmodium vivax infection and identification of candidate immunogenic rhoptry-associated membrane antigen (RAMA). *J. Proteomics* 102, 66–82. doi: 10.1016/J.JPROT.2014.02.029

Lustigman, S., Prichard, R. K., Gazzinelli, A., Grant, W. N., Boatin, B. A., McCarthy, J. S., et al. (2012). A research agenda for helminth diseases of humans: the problem of helminthiases. *PLoS Negl. Trop. Dis.* 6, e1582. doi: 10.1371/JOURNAL.PNTD.0001582

Marcilla, A., Martin-Jaular, L., Trelis, M., de Menezes-Neto, A., Osuna, A., Bernal, D., et al. (2014). Extracellular vesicles in parasitic diseases. *J. Extracell Vesicles* 3, 25040. doi: 10.3402/JEV.V3.25040

Martín-Jaular, L., de Menezes-Neto, A., Monguió-Tortajada, M., Elizalde-Torrent, A., Díaz-Varela, M., Fernández-Becerra, C., et al. (2016). Spleen-dependent immune protection elicited by CpG adjuvanted reticulocyte-derived exosomes from malaria infection is associated with changes in T cell subsets' distribution. *Front. Cell Dev. Biol.* 4. doi: 10.3389/FCELL.2016.00131/FULL

Martin-Jaular, L., Nakayasu, E. S., Ferrer, M., Almeida, I. C., and del Portillo, H. A. (2011). Exosomes from plasmodium yoelii-infected reticulocytes protect mice from lethal infections. *PLoS One* 6, e26588. doi: 10.1371/JOURNAL.PONE.0026588

Mason, C. P., and Tarr, A. W. (2015). Human lectins and their roles in viral infections. *Molecules* 20, 2229–2271. doi: 10.3390/MOLECULES20022229

Mathieu, M., Martin-Jaular, L., Lavieu, G., and Théry, C. (2019). Specificities of secretion and uptake of exosomes and other extracellular vesicles for cell-to-cell communication. *Nat. Cell Biol.* 21, 9–17. doi: 10.1038/s41556-018-0250-9

Minigo, G., Woodberry, T., Piera, K. A., Salwati, E., Tjitra, E., Kenangalem, E., et al. (2009). Parasite-dependent expansion of TNF receptor II-positive regulatory T cells with enhanced suppressive activity in adults with severe malaria. *PLoS Pathog.* 5, e1000402. doi: 10.1371/JOURNAL.PPAT.1000402

Ministerio de Salud y Protección Social, U. de A (2015). *Encuesta nacional de parasitismo intestinal en población escolar 2012 – 2014. 1st Edn* (Medellín, Colombia: Ministerio de la Protección Social). U. de A. Ministerio de Salud y Protección Social.

Miyabe, Y., Miyabe, C., and Luster, A. D. (2017). LTB4 and BLT1 in inflammatory arthritis. *Semin. Immunol.* 33, 52–57. doi: 10.1016/J.SMIM.2017.09.009

Moellmer, S. A., Puy, C., and McCarty, O. J. T. (2024). Biology of factor XI. *Blood* 143, 1445–1454. doi: 10.1182/BLOOD.2023020719

Moro, L., Bardají, A., Macete, E., Barrios, D., Morales-Prieto, D. M., España, C., et al. (2016). Placental microparticles and microRNAs in pregnant women with plasmodium falciparum or HIV infection. *PLoS One* 11, e0146361. doi: 10.1371/journal.pone.0146361

Mpairwe, H., Tweyongyere, R., and Elliott, A. (2014). Pregnancy and helminth infections. *Parasite Immunol.* 36, 328–337. doi: 10.1111/pim.12101

Murray, C. J. L., Ortblad, K. F., Guinovart, C., Lim, S. S., Wolock, T. M., Roberts, D. A., et al. (2014). Global, regional, and national incidence and mortality for HIV, tuberculosis, and malaria during 1990-2013: a systematic analysis for the Global Burden of Disease Study 2013. *Lancet* 384, 1005–1070. doi: 10.1016/S0140-6736(14)60844-8

Nantakomol, D., Dondorp, A. M., Krudsood, S., Udomsangpetch, R., Pattanapanyasat, K., Combes, V., et al. (2011). Circulating red cell-derived microparticles in human malaria. *J. Infect. Dis.* 203, 700–706. doi: 10.1093/infdis/jiq104

Pathan, M., Fonseka, P., Chitti, S. V., Kang, T., Sanwlani, R., Van Deun, J., et al. (2019). Vesiclepedia 2019: a compendium of RNA, proteins, lipids and metabolites in extracellular vesicles. *Nucleic Acids Res.* 47, D516–D519. doi: 10.1093/NAR/GKY1029

Perez Botero, J., Coon, L. M., Majerus, J. A., Chen, D., and Pruthi, R. K. (2018). Factor IX gene (F9) genotyping trends and spectrum of mutations identified: A reference laboratory experience. *Semin. Thromb. Hemost* 44, 287–292. doi: 10.1055/S-0037-1605567

Rayner, J. C., Huber, C. S., Feldman, D., Ingravallo, P., Galinski, M. R., and Barnwell, J. W. (2004). Plasmodium vivax merozoite surface protein PvMSP-3β is radically polymorphic through mutation and large insertions and deletions. *Infection Genet. Evol.* 4, 309–319. doi: 10.1016/j.meegid.2004.03.003

Rogerson, S. J., Hviid, L., Duffy, P. E., Leke, R. F., and Taylor, D. W. (2007a). Malaria in pregnancy: pathogenesis and immunity. *Lancet Infect. Dis.* 7, 105–117. doi: 10.1016/S1473-3099(07)70022-1

Rogerson, S. J., Mwapasa, V., and Meshnick, S. R. (2007b). Malaria in pregnancy: linking immunity and pathogenesis to prevention. *Am. J. Trop. Med. Hyg* 77, 14–22. doi: 10.4269/AJTMH.77.6.SUPPL.14

Saito, S., Nakashima, A., Shima, T., and Ito, M. (2010). Th1/Th2/Th17 and regulatory T-cell paradigm in pregnancy. *Am. J. Reprod. Immunol.* 63, 601–610. doi: 10.1111/J.1600-0897.2010.00852.X

Sampaio, N. G., Cheng, L., and Eriksson, E. M. (2017). The role of extracellular vesicles in malaria biology and pathogenesis. *Malar J.* 16, 245. doi: 10.1186/S12936-017-1891-Z

Sánchez-López, C. M., González-Arce, A., Ramírez-Toledo, V., Bernal, D., and Marcilla, A. (2024). Unraveling new players in helminth pathology: extracellular vesicles from *Fasciola hepatica* and *Dicrocoelium dendriticum* exert different effects on hepatic stellate cells and hepatocytes. *Int. J. Parasitol.* 54, 617–634. doi: 10.1016/j.ijpara.2024.06.002

Schorey, J. S., Cheng, Y., Singh, P. P., and Smith, V. L. (2015). Exosomes and other extracellular vesicles in host-pathogen interactions. *EMBO Rep.* 16, 24–43. doi: 10.15252/EMBR.201439363

Shiroishi, M., Kuroki, K., Ose, T., Rasubala, L., Shiratori, I., Arase, H., et al. (2006). Efficient leukocyte Ig-like receptor signaling and crystal structure of disulfide-linked HLA-G dimer. *J. Biol. Chem.* 281, 10439–10447. doi: 10.1074/JBC.M512305200

Shiroishi, M., Tsumoto, K., Amano, K., Shirakihara, Y., Colonna, M., Braud, V. M., et al. (2003). Human inhibitory receptors Ig-like transcript 2 (ILT2) and ILT4 compete with CD8 for MHC class I binding and bind preferentially to HLA-G. *Proc. Natl. Acad. Sci. U.S.A.* 100, 8856–8861. doi: 10.1073/PNAS.1431057100

Sisquella, X., Ofir-Birin, Y., Pimentel, M. A., Cheng, L., Abou Karam, P., Sampaio, N. G., et al. (2017). Malaria parasite DNA-harbouring vesicles activate cytosolic immune sensors. *Nat. Commun.* 8, 1985. doi: 10.1038/s41467-017-02083-1

Sow, D., Parola, P., Sylla, K., Ndiaye, M., Delaunay, P., Halfon, P., et al. (2017). Performance of real-time polymerase chain reaction assays for the detection of 20 gastrointestinal parasites in clinical samples from Senegal. *Am. J. Trop. Med. Hyg* 97, 173. doi: 10.4269/AJTMH.16-0781

Stam, J., Bartel, S., Bischoff, R., and Wolters, J. C. (2021). Isolation of extracellular vesicles with combined enrichment methods. *J. Chromatogr B Analyt Technol. BioMed. Life Sci.* 1169, 122604. doi: 10.1016/j.jchromb.2021.122604

Toda, H., Diaz-Varela, M., Segui-Barber, J., Roobsoong, W., Baro, B., Garcia-Silva, S., et al. (2020). Plasma-derived extracellular vesicles from Plasmodium vivax patients signal spleen fibroblasts via NF-kB facilitating parasite cytoadherence. *Nat. Commun.* 11, 2761. doi: 10.1038/s41467-020-16337-y

Utzinger, J., Becker, S. L., Knopp, S., Blum, J., Neumayr, A. L., Keiser, J., et al. (2012). Neglected tropical diseases: diagnosis, clinical management, treatment and control. *Swiss Med. Wkly* 142, w13727. doi: 10.4414/SMW.2012.13727

van Niel, G., Carter, D. R. F., Clayton, A., Lambert, D. W., Raposo, G., and Vader, P. (2022). Challenges and directions in studying cell-cell communication by extracellular vesicles. *Nat. Rev. Mol. Cell Biol.* 23, 369–382. doi: 10.1038/S41580-022-00460-3

Wammes, L. J., Wiria, A. E., Toenhake, C. G., Hamid, F., Liu, K. Y., Suryani, H., et al. (2013). Asymptomatic plasmodial infection is associated with increased tumor necrosis factor receptor II-expressing regulatory T cells and suppressed type 2 immune responses. *J. Infect. Dis.* 207, 1590–1599. doi: 10.1093/INFDIS/JIT058

Warncke, J. D., Vakonakis, I., and Beck, H.-P. (2016). Plasmodium helical interspersed subtelomeric (PHIST) proteins, at the center of host cell remodeling. *Microbiol. Mol. Biol. Rev.* 80, 905. doi: 10.1128/MMBR.00014-16

White, N. J., Pukrittayakamee, S., Hien, T. T., Faiz, M. A., Mokuolu, O. A., and Dondorp, A. M. (2014). Malaria. *Lancet* 383, 723–735. doi: 10.1016/S0140-6736(13)60024-0

Wilairatana, P., Mahannop, P., Tussato, T., Hayeedoloh, I., Boonhok, R., Klangbud, W. K., et al. (2021). C-reactive protein as an early biomarker for malaria infection and monitoring of malaria severity: a meta-analysis. *Sci. Rep.* 11, 22033. doi: 10.1038/S41598-021-01556-0

World Health Organization (2023). *Global Malaria Programme*. Available online at: https://www.who.int/teams/global-malaria-programme/case-management/diagnosis/microscopy (Accessed August 8, 2024).

Yáñez-Mó, M., Siljander, P. R. M., Andreu, Z., Zavec, A. B., Borràs, F. E., Buzas, E. I., et al. (2015). Biological properties of extracellular vesicles and their physiological functions. *J. Extracell Vesicles* 4, 27066. doi: 10.3402/JEV.V4.27066